REPORT DOCUMENTATION PAGE

AFRL-SR-AR-TR-02-

0387

1. AGENCY USE ONLY (Leave blank)	2. REPORT DATE	3. REPORT TYPE AND DATES COVERED
	August 02, 2002	Fianl report (01March2000-31 July 2001)

4. TITLE AND SUBTITLE

DYNAMIC ANALYSIS OF ADAPTIVE STRUCTURES WITH EMBEDDED COMPLIANT MECHANISMS

5. FUNDING NUMBERS

F49620-00-1-0178

6. AUTHOR(S)

Sridhar Kota

7. PERFORMING ORGANIZATION NAME(S) AND ADDRESS(ES)

Department of Mechanical Engineering
University of Michigan, Ann Arbor
MI 48109-2125

8. PERFORMING ORGANIZATION REPORT NUMBER

9. SPONSORING / MONITORING AGENCY NAME(S) AND ADDRESS(ES)

Air Force Office of Scientific Research

10. SPONSORING / MONITORING AGENCY REPORT NUMBER

11. SUPPLEMENTARY NOTES

12a. DISTRIBUTION / AVAILABILITY STATEMENT

Approved for public release;
distribution unlimited.

12b. DISTRIBUTION CODE

13. ABSTRACT ***(Maximum 200 Words)***

A systematic method for dynamic analysis of compliant mechanisms was developed including basic formulations for natural frequencies, modes, dynamic response, and frequency characteristics. Methods for design sensitivity analysis were developed to investigate the effect of various design parameters on the dynamic performance of compliant mechanisms. A micro compliant stroke amplifier mechanism, for MEMS actuator application, is presented in this report, as a design example, to demonstrate significant differences between static and dynamic performance of compliant mechanisms. This general-purpose methodology can be applied to adaptive structures for aerospace applications. The methodology was implemented in MATLAB with user-friendly graphical interface.

14. SUBJECT TERMS

15. NUMBER OF PAGES

20

16. PRICE CODE

17. SECURITY CLASSIFICATION OF REPORT	18. SECURITY CLASSIFICATION OF THIS PAGE	19. SECURITY CLASSIFICATION OF ABSTRACT	20. LIMITATION OF ABSTRACT
NONE	NONE	NONE	NONE

FINAL REPORT

DYNAMIC ANALYSIS OF ADAPTIVE STRUCTURES WITH EMBEDDED COMPLIANT MECHANISMS

AFOSR CONTRACT NUMBER: F49620-00-1-0178

PROJECT DURATION 3/1/00-7/31/01

SRIDHAR KOTA

PROFESSOR OF MECHANICAL ENGINEERING

THE UNIVERSITY OF MICHIGAN, ANN ARBOR, MI 48109

(734)-936-0357, FAX 734-647-3170, EMAIL kota@umich.edu

July 2002

DYNAMIC ANALYSIS OF ADAPTIVE STRUCTURES WITH EMBEDDED COMPLIANT MECHANISMS

1.0 Objectives

Development of analytical formulations to predict the dynamic performance of compliant structures.

2.0 Status of Effort

A systematic method for dynamic analysis of compliant mechanisms was developed including basic formulations for natural frequencies, modes, dynamic response, and frequency characteristics. Methods for design sensitivity analysis were developed to investigate the effect of various design parameters on the dynamic performance of compliant mechanisms. A micro compliant stroke amplifier mechanism, for MEMS actuator application, is presented in this report, as a design example, to demonstrate significant differences between static and dynamic performance of compliant mechanisms. This general-purpose methodology can be applied to adaptive structures for aerospace applications. The methodology was implemented in MATLAB with user-friendly graphical interface.

In our current AFOSR contract, we are developing analytical formulations for synthesis of compliant structures under deformation-dependent pressure loads (air loads).This report will focus on work carried out on dynamic analysis under the contract number F49620-00-1-0178

3. 0 Summary of Accomplishments

3.1 Basic Research

The PIs, S. Kota, and N. Kikuchi have developed and tested the fundamental formulations for the design of compliant mechanisms including the following tasks:

- (1996-1998)Given a set of functional requirements; that is forces and desired displacements, determine an optimized topology (configuration) of a complaint mechanism.
- (1996-1998)Given the initial and final shape of a flexible body, determine the optimal topology of a complaint mechanism that can produce the desired shape change using a single actuator - external loading was not taken in to account in this preliminary investigation.
- (1997-1999)Given the topology of a compliant mechanism, determine the optimum size and shape of all members of the mechanism such that energy efficiency is maximized.
- (1999-2000)Dynamic analysis of compliant mechanisms and determination of sensitivity coefficients (THIS REPORT)

The results from the work supported by the AFOSR contract are published in the following journal articles

- S. Kota, J. Hetrick, Z. Li, L. Saggere, "Tailoring Unconventional Actuators Using Compliant Transmissions: Design Methods and Applications," *IEEE/ASME Transactions on Mechatronics*, Vol. 4, Number 4, pp 396-408, December 1999.
- Kota S., Hetrick J., Li Z., Rodgers S., Krygowski T., "Synthesizing High-Performance Compliant Stroke Amplification Systems for MEMS, Proc. of the Thirteenth Annual International Conference on Micro Electro Mechanical Systems, Miyazaki, Japan, Jan. 2000.
- S. Kota, J. Joo, Zhe Li, et al. Design of Compliant Mechanisms: Applications to MEMS, Analog Integrated Circuits and Signal Processing-An International Journal, 29, 7-15, 2001. Kluwer Academic Publications.
- Li Z., and S. Kota, "Dynamic Analysis of Compliant Mechanisms", Proceedings of DETC 2002, 27th Biannual Mechanisms and Robotics Conference, September 29 – October 2, Montreal, Canada

3.2 Technology Transition

1. Under a contract with WPAFB, the PI S. Kota has designed, fabricated and tested a 3-foot wing section of NACA63418 profile embedded with compliant mechanisms. A low-speed wind tunnel test revealed significant improvement in lift coefficient as the leading camber is changed.

2. An STTR contract with AFOSR is underway to develop high-frequency vortex generator for active flow control. The device utilizes a compliant stroke amplification mechanism in conjunction with a piezo actuator. The project is in collaboration with Lockheed Martin Tactical Aircraft Systems.

3. In collaboration with Sandia National Labs, we developed novel compliant stroke amplification mechanisms that are integrated with electrostatic linear actuators. The result was a 220-fold improvement in force per unit area (Figure 2A).

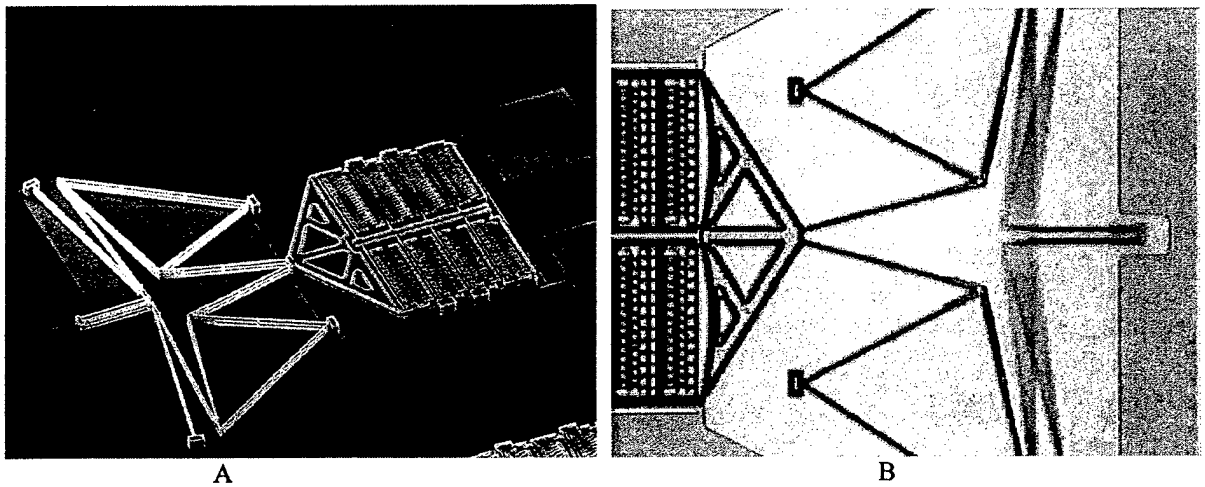

A B

A 20X Complaint Stroke Multiplier integrated with electrostatic linear actuator. A. Manufactured using Sandia National Lab's advanced 5-level surface micromachining technology. B. The device operating at 27KHz, tested at 10^{10} cycles without failure.

3.3 Inventions and Patent Disclosures

The following patent application was filed (work under previous AFSOR contract F49620-96-1-0205.

1. Joel Hetrick, Sridhar Kota, Displacement Amplification Structure, Serial number 09/658,058, Filed September 2000. UM reference number 2115-001740.

3.4 Benefits to AFSOR

- Lays a scientific foundation for designing multifunctional structures with embedded actuation for applications to smart structures and MEMS.
- Scalable concepts in adaptive airfoils.
- Expand the scope and application of present day smart actuators such as PZTs and SMAs by integrating a compliant transmission with an actuator to generate desired force-displacement characteristics.

4.0 Personnel Supported

Sridhar Kota, PI/PD Professor of Mechanical Engineering, University of Michigan, Ann Arbor.

Dr. Zhe Li, Research Associate, Mechanical Engineering, University of Michigan, Ann Arbor.

Doctoral Students

Jin Yong Joo. Dr. Joo is nowa researcher at AFRL, Wright PattersonAFB.

Ms. Kerr-Jia Lu, Mechanical Engineering, University of Michigan, Ann Arbor.

C034442
L closed
3/8/00

5.0 TECHNICAL REPORT

5.1 Introduction

Designing a compliant mechanism for a specific application can be a complex problem with many considerations. The basic trade-off is between the flexibility to achieve deformed motion and the rigidity to sustain external load. Many researchers have addressed proposed various synthesis techniques for creating a viable compliant mechanism [1-11] including topology and shape optimization methods. Many of these methods for topology and dimensional synthesis are based on kinetostatic design specifications and do not consider the dynamic effects in the design stage. Therefore, the resulting designs are valid for static or low frequency applications. The dynamic effects can be significant and for instance, a complaint mechanism may exhibit a very different mechanical advantage at high frequencies compared to what it was designed for static situations. The synthesis algorithms should, ideally, account for operating frequency before generating an appropriate topology and dimensions. Towards this goal, we first developed analysis formulations to investigate the dynamic behavior of compliant mechanisms.

In this report we present a systematic method for the dynamic analysis of compliant mechanisms including differential equations of motion, formulae for natural frequencies and modes, dynamic responses, dynamic compliance, and sensitivity analysis. A design example demonstrates the significance and the effectiveness of these methods in improving the dynamic behavior. Although the basic formulations developed in this work are well understood and reported in the published literature, we tailored the formulations for elastic structures and the report highlights the significance of dynamic response of compliant mechanisms and the need to account for the same during the design phase. Additionally, methods to carry out sensitivity analysis are developed to investigate the effect of various design parameters on the dynamic performance of compliant mechanisms. In the next section, we present the basic dynamic analysis formulations.

5.2 Dynamic Equations of Compliant Mechanisms

The dynamic differential equations of a compliant mechanism can be derived using the finite element method and take the form of

$$[M]_{n\times n}\{\ddot{D}\}_{n\times 1} + [C]_{n\times n}\{\dot{D}\}_{n\times 1} + [K]_{n\times n}\{D\}_{n\times 1} = \{R\}_{n\times 1} \qquad (1)$$

where $[M]$, $[C]$ and $[K]$ are system mass, damping and stiffness matrix respectively; $\{D\}$ is the set of generalized coordinates representing the translation and rotation deformations at each element node in global coordinate system; $\{R\}$ is the set of generalized external forces corresponding to $\{D\}$; n is the number of the generalized coordinates (elastic degrees of freedom of the mechanism). If we use frame elements shown in Fig. 1 in the formulation, the element mass matrix and stiffness matrix can be written as Eq. (2) and Eq. (3).

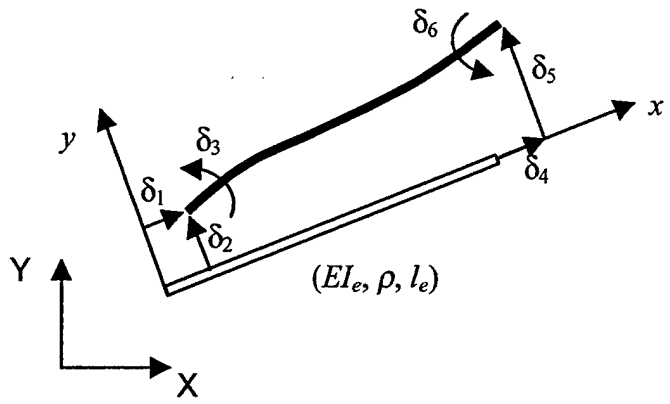

Figure 1 Planar frame element in which EI_e is the bending stiffness (E is the modulus of elasticity of the material, I_e is the moment of inertia), ρ is the material density, l_e is the original length of the element. δ_i (i=1,2,...6) are nodal displacements expressed in local coordinate system (x, y).

$$[m]_e=\begin{bmatrix} 2a & 0 & 0 & a & 0 & 0 \\ & 156b & 22l_eb & 0 & 54b & -13l_eb \\ & & 4l_e^2b & 0 & 13l_eb & -3l_e^2b \\ & & & 2a & 0 & 0 \\ & Symmetric & & & 156b & -22l_eb \\ & & & & & 4l_e^2b \end{bmatrix} \tag{2}$$

$$[k]_e=\begin{bmatrix} \frac{EA_e}{l_e} & 0 & 0 & \frac{-EA_e}{l_e} & 0 & 0 \\ & \frac{12EI_e}{l_e^3} & \frac{6EI_e}{l_e^2} & 0 & \frac{-12EI_e}{l_e^3} & \frac{6EI_e}{l_e^2} \\ & & \frac{4EI_e}{l_e} & 0 & \frac{-6EI_e}{l_e^2} & \frac{2EI_e}{l_e} \\ & & & \frac{EA_e}{l_e} & 0 & 0 \\ & Symmetric & & & \frac{12EI_e}{l_e^3} & \frac{-6EI_e}{l_e^2} \\ & & & & & \frac{4EI_e}{l_e} \end{bmatrix} \tag{3}$$

where $a = \frac{\rho A_e l_e}{6}$, $b = \frac{\rho A_e l_e}{420}$, A_e is the cross sectional area of the element. The mass and stiffness matrices of the element are derived from the kinetic energy and strain energy expressions as follows:

$$\left\{\frac{d}{dt}\left(\frac{\partial T}{\partial \dot{\delta}}\right) - \frac{\partial T}{\partial \delta}\right\} = [m]_e \{\ddot{\delta}\} \tag{4}$$

$$\left\{\frac{\partial U}{\partial \delta}\right\} = [k]_e \{\delta\} \tag{5}$$

where T is the kinetic energy and U is the strain energy of the element; $\{\delta\} = [\delta_1\ \delta_2\ \delta_3\ \delta_4\ \delta_5\ \delta_6]^T$, are the linear and angular deformations of the node at the element local coordinate system. Detailed derivations can be readily found in finite element textbooks [12, 13]. Typically, a compliant mechanism is discretized into many elements as in finite element analysis. Each element is associated with a mass and a stiffness matrix as Eq. (2) and (3). Each element has its own local coordinate system. We combine the element mass and stiffness matrices of all elements and perform coordinate transformations necessary to transform the element local coordinate system to global coordinate system. This gives the system mass [M] and stiffness [K] matrices. Capturing the damping characteristics in a compliant system is not so straightforward. Even though, in many applications, damping may be small but its effect on the system stability and dynamic response, especially in the resonance region, can be significant. The damping matrix [C] can be written as a linear combination of the mass and stiffness matrices [14] and is called proportional damping [C] which is expressed as

$$[C] = \alpha[M] + \beta[K] \tag{6}$$

where α and β are two positive coefficients which are usually determined by experiment. An alternate method [15] of representing the damping matrix is expressing [C] as

$$[C] = [M][C'] \tag{7}$$

The element of [C'] is defined as $C'_{ij} = 2\zeta\left(signK_{ij}\right)\left(K_{ij}/M_{ij}\right)^{\frac{1}{2}}$, where $signK_{ij} = \left(K_{ij}/\left|K_{ij}\right|\right)$, K_{ij} and M_{ij} are the elements of [K] and [M], ζ is the damping ratio of the material.

The generalized force in a frame element is defined as

$$R_i^e = \sum_{j=1}^{m}\left(\mathrm{F}_{xj}\frac{\partial \mathrm{x}_j}{\partial \delta_i} + \mathrm{F}_{yj}\frac{\partial \mathrm{y}_j}{\partial \delta_i} + \mathrm{M}_{\theta j}\frac{\partial \theta_j}{\partial \delta_i}\right) \qquad (i=1,2,\ldots,6) \tag{8}$$

where F_j and M_j are the jth external force and moment on the element acting at $(\mathrm{x}_j, \mathrm{y}_j)$, and m is the number of the external forces acting on the element. The element generalized forces $\{R\}_e =$

$[R_1^e \ R_2^e \ R_3^e \ R_4^e \ R_5^e \ R_6^e]^T$, are then combined to form the system generalized force {R}. The second order ordinary differential equations of motion of the system, Eq. (1), can be directly integrated with a numerical method such as Runge-Kutta method.

Another commonly used method to solve Eq. (1) is the so-called modal analysis technique. This method first decouples the Eq. (1) with modal matrix, [Φ], into

$$\ddot{Z}_i + 2\xi_i \omega_i \dot{Z}_i + \omega_i^2 Z_i = P_i \qquad (i=1, 2, \ldots, n) \tag{9}$$

where Z_i and P_i are the ith normalized coordinate and force, ξ_i is the damping coefficient added to the decoupled equations (typically ξ_i=0.01-0.2), and ω_i is the ith circular natural frequency of the system. Once the normalized coordinates {Z} are solved from Eq. (9), the node deformation {D} can be determined by the transformation

$$\{D\} = [\Phi]\{Z\} \tag{10}$$

The determination of the modal matrix and natural frequency will be presented in next section. Dynamic analysis and synthesis of compliant mechanisms are based on the solution of the differential equations of motion of the system.

5.3 Dynamic Analysis

5.3.1 Natural frequencies and natural modes

In order to obtain the natural frequencies and natural modes of a system, undamped free vibration equation is used because the damping has very little influence on the natural frequencies of a system. From the free vibration of the system, we have the following modal equation

$$([K] - \lambda_i [M])\{X_i\} = \{0\} \qquad (i=1, 2, \ldots, n) \tag{11}$$

The condition of non-zero solution of Eq. (11) is

$$|([K] - \lambda_i [M])| = 0 \qquad (i=1, 2, \ldots, n) \tag{12}$$

From Eq. (12), we can obtain the eigenvalues λ_i (i=1, 2,...,n) of the system and $\lambda_i = \omega_i^2$. The cyclic frequency $f_i = \omega_i / 2\pi$ Hertz. By substituting each eigenvalue λ_i into Eq. (11), the eigenvector $\{X_i\}$ or the ith natural mode of the system can be determined. The modal matrix is defined as

$$[\Phi] = [\{X_1\} \ \{X_2\} \ \ldots \ \{X_n\}] \tag{13}$$

It can be used to decouple the differential equations of the system.

5.3.2 Time responses

The nodal displacements and rotations $\{D\}$ of the compliant mechanism can be obtained by solving the dynamic equation (1) under certain excitation and load conditions. The nodal velocity and acceleration, $\{\dot{D}\}$ and $\{\ddot{D}\}$ can also be solved directly through Eq. (1). The deformation within an element can be determined by an interpolation technique. If we use linear interpolation to approximate the axial deformation, and use third-order Hermite interpolation [12] to approximate the bending deformation, the deformation at any point x within the element can be expressed as

$$\begin{aligned} u &= \left(1-\frac{x}{l_e}\right)\delta_1 + \frac{x}{l_e}\delta_4 \\ v &= \left(1-\frac{3x^2}{l_e^2}+\frac{2x^3}{l_e^3}\right)\delta_2 + \left(x-\frac{2x^2}{l_e}+\frac{x^3}{l_e^2}\right)\delta_3 + \left(\frac{3x^2}{l_e^2}-\frac{2x^3}{l_e^3}\right)\delta_5 + \left(-\frac{x^2}{l_e}+\frac{x^3}{l_e^2}\right)\delta_6 \end{aligned} \tag{14}$$

where u and v are deformations along x and y directions measured in the element local coordinate system. The normal bending stress in the element is given by

$$\sigma_x = -\frac{E\dfrac{\partial^2 v}{\partial x^2}y}{\left[1+\left(\dfrac{\partial v}{\partial x}\right)^2\right]^{3/2}} \tag{15}$$

where y is the distance of a point in the beam cross-section measured from the neutral surface. The deformations and stresses in the compliant mechanism vary as a function of the independent variable t (time).

5.3.3 Frequency characteristics

Modal testing or hammer tap testing theory has been successfully used for calculating the frequency spectrum of a structure or a machine tool [16, 17]. It is also applicable to compliant mechanisms. Basic frequency spectrum includes the amplitude-frequency characteristic (dynamic compliance) and the phase-frequency characteristic of a system. Frequency characteristic analysis is important to gain an understanding of the dynamic performance of a compliant mechanism especially when it has a wide range of working frequency. The resonance phenomenon can be examined through the amplitude-frequency characteristics of the system. Even if the amplitude of the system output matches the design specification, the phase angle between the input and output of the system may not meet the desired performance. Mathematically, suppose the input force acting on the compliant mechanism is $F(t)$, the output displacement is $Y(t)$, then the transfer function $G(j\omega)$ of the system is defined as

$$G(j\omega)=\frac{\int_0^T Y(t)e^{-jwt}dt}{\int_0^T F(t)e^{-jwt}dt}=\frac{E_Y(j\omega)}{E_F(j\omega)} \tag{16}$$

where $E_F(j\omega)$ and $E_Y(j\omega)$ are complex energy spectrums of the input force and output displacement. The integrations are the Fourier transform expressions and can be calculated by FFT algorithm [18]. Dividing the complex energy spectrum by the integration time T, we obtain the complex power spectra:

$$\begin{aligned} S_F(j\omega)&=\frac{1}{T}E_F(j\omega)\\ S_Y(j\omega)&=\frac{1}{T}E_Y(j\omega) \end{aligned} \tag{17}$$

After expansion with the complex conjugate, the transfer function can be expressed as

$$\begin{aligned} G(j\omega)&=\frac{S_Y(j\omega)}{S_F(j\omega)}=\frac{S_Y(j\omega)\cdot S_F^*(j\omega)}{S_F(j\omega)\cdot S_F^*(j\omega)}=\frac{S_{YF}(j\omega)}{S_{FF}(\omega)}\\ &=\frac{\mathrm{Re}\{S_{YF}(j\omega)\}+j\,\mathrm{Im}\{S_{YF}(j\omega)\}}{S_{FF}(\omega)} \end{aligned} \tag{18}$$

where $S_F^*(j\omega)$ is the complex conjugate of $S_F(j\omega)$, $S_{FF}(j\omega)$ is the auto-power spectrum (real), $S_{YF}(j\omega)$ is the cross-power spectrum (complex). The magnitude of $G(j\omega)$ is the dynamic compliance of the system. The phase angle between the input force and output displacement is defined as

$$\phi=\arctan\frac{\mathrm{Im}\{G(j\omega)\}}{\mathrm{Re}\{G(j\omega)\}} \tag{19}$$

5.3.4 Sensitivities

Sensitivity analysis is an effective way to predict the influence of various physical parameters on the performance of a compliant mechanism. It can be used very effectively to guide the redesign efforts in tuning the design parameters for desired dynamic performance. Minimizing the sensitivity of the response to system parameters can make the design robust and insensitive to manufacturing errors or overload. The sensitivity formulae of the natural frequency and vibration mode with respect to a certain physical parameter s of the system are derived as follows. From Eq. (11) we have

$$\{X_i\}^T[S_i]\{X_i\}=0 \tag{20}$$

where $[S_i]=[K]-\omega_i^2[M]$. Differentiating Eq. (20) with respect to s,

$$\frac{\partial\{X_i\}^T}{\partial s}[S_i]\{X_i\}+\{X_i\}^T\frac{\partial[S_i]}{\partial s}\{X_i\}+\{X_i\}^T[S_i]\frac{\partial\{X_i\}}{\partial s}=0 \tag{21}$$

By employing the following equalities
$[S_i]\{X_i\}=\{0\}_{n\times 1}$, $\{X_i\}^T[S_i]=\{0\}_{1\times n}$, and $\{X_i\}^T[M]\{X_i\}=1$ [14], and rearranging the terms, the sensitivity of the natural frequency to the design variable s can be derived from Eq. (21) as

$$\frac{\partial\omega_i}{\partial s}=\frac{1}{2}\omega_i^{-1}\{X_i\}^T\frac{\partial[K]}{\partial s}\{X_i\}-\frac{1}{2}\omega_i\{X_i\}^T\frac{\partial[M]}{\partial s}\{X_i\} \tag{22}$$

The sensitivity of natural mode can be derived in a similar way starting with Eq. (11) and is given as

$$\frac{\partial\{X_i\}}{\partial s}=-\left([K]-\omega_i^2[M]\right)^{-1}\left\{\frac{\partial[K]}{\partial s}-2\omega_i\frac{\partial\omega_i}{\partial s}[M]-\omega_i^2\frac{\partial[M]}{\partial s}\right\}\{X_i\} \tag{23}$$

where the physical parameter s of the system can be the mass, bending stiffness, length, or cross-section of an element. The values of the natural frequency ω_i and mode $\{X_i\}$ can be obtained from Eq. (12) and Eq. (11).

5.4 Dynamic Performance of a Compliant Stroke Multiplier

A stroke amplification compliant mechanism is taken as a design example to illustrate the dynamic performance of a compliant mechanism that was designed to meet only the kinetostatic requirements. The mechanism was originally designed for motion amplification application in the MEMS domain and was fabricated at Sandia National Labs (see Fig. 2). By combining a stroke amplifier, with a very short stroke, high force and compact linear actuator, Sandia Microsystems group was able to generate 220 times more force per unit area compared to their earlier version without the stroke amplifier. The design shown in Fig. 2 was originally optimized for maximum energy efficiency and to meet kinetostatic input/out put force-displacement requirements. The goal was to design a 12X stroke multiplier for operation at high frequencies (500Hz and above). The design optimization only accounted for static behavior. From the design results obtained by the energy efficiency method [10], we determined that the compliant multiplier has the geometric advantage (GA) = 12.1, and a 180 degree phase angle between the output and the input. That is the input and the output are in opposite moving directions. The right-half of the symmetric compliant mechanism is shown in Fig. 3. This mechanism is discretized into 32 planar frame elements where m_i and EI_i are mass and bending stiffness of the element i. The total number of nodal degrees of freedom is 38 for the mechanism shown in 3. It should be noted that the dynamic performance of the half mechanism is the same as the whole mechanism because both the mass and the stiffness of the half mechanism are reduced one half compared with the whole mechanism. Since the focus was mainly on understanding the behavior of the compliant mechanism, the mass of the micro actuator is not accounted for in the computation. To verify the system performance, the actuator mass and the load must be taken in to consideration.

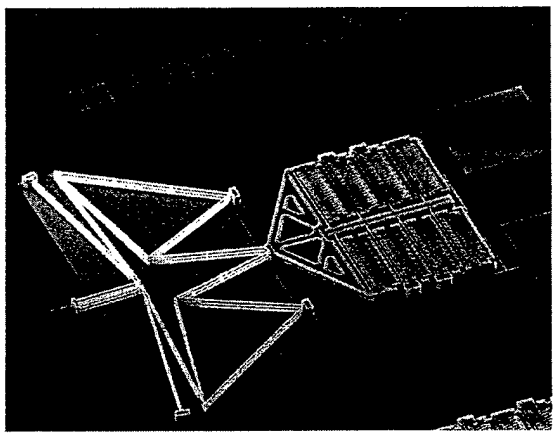

Figure 2 Micrograph of a stroke-amplification mechanism integrated with an linear electrostatic actuator. The device was fabricated at the Sandia National Labs using 5-level surface micro machining technology called SUMMiT-V. The overall size (footprint) of the assembly shown here is approximately 300 μm x 500 μm. U.S. Patent number 6,175,170 B1.

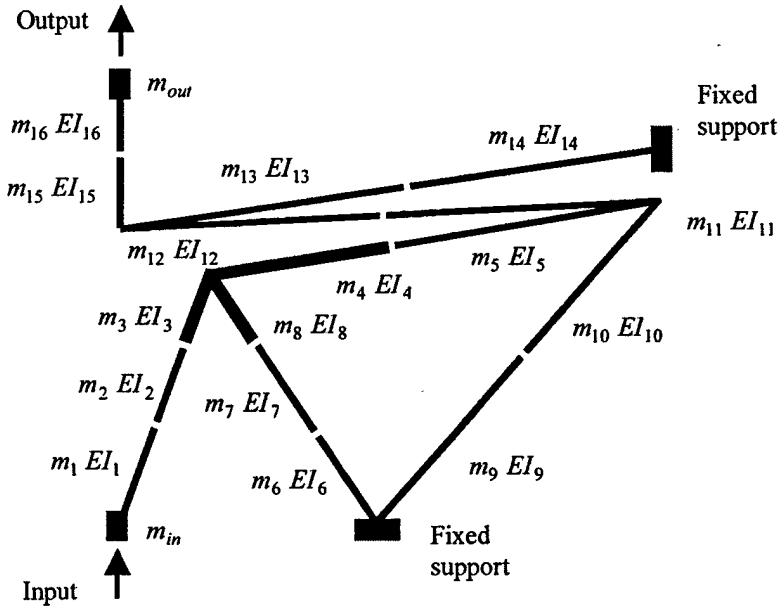

Figure 3 One-half model of a stroke amplification compliant mechanism.

The dynamic differential equations of the mechanism take the form of Eq. (1) where n=38. The computed natural frequencies of the compliant mechanism are:

$$f_1 = 3883.24\,(\text{Hertz}), \qquad f_2 = 124{,}030.12\,(\text{Hertz}),$$
$$f_3 = 155{,}498.66\,(\text{Hertz}), \quad f_4 = 182{,}115.04\,(\text{Hertz}),$$
$$\Lambda$$

Because the working frequency of the mechanism is in the range of [500, 5000](Hertz), according to the values of natural frequencies, it can be estimated that the deformation shape of the compliant mechanism is dominated by the first natural mode as shown in Fig. 4, where the red line is the deformed position.

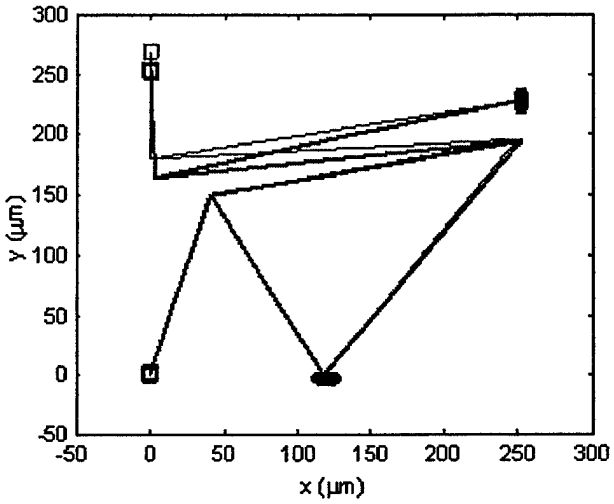

Figure 4: The first natural mode of the compliant mechanism.

Suppose a driving force $F = 13\sin(\omega_{in} t)\,(\mu\text{N})$ is applied to the input port, where ω_{in} (rad/s) is the operation speed. Although the driving force is a standard sine function, the time history of the output displacement may be not an exact sine function. Figure 5 is a snap shot of dynamic behavior between 16 and 24 motion cycles as the device is operating at 3000 Hz. Note that the displacement (stroke) amplitude changes with each motion cycle. This phenomenon reflects the dynamic complexity of the compliant mechanism because the amplitude as well as the phase of the response changes with the actuation frequency.

The amplitude-frequency characteristic of the output displacement is shown in Fig. 6(a), from which a non-linear relationship of the amplitude versus input frequency can be seen. In Fig. 6(a), the frequency ratio refers to the ratio of the input frequency over the fundamental frequency. Likewise, the displacement ratio refers to the amplitude of the output displacement over the static displacement, which is equal to $24.13\,(\mu\text{m})$. The maximum value of the output displacement at a given operation frequency can be quantitatively determined from the amplitude-frequency characteristic curve.

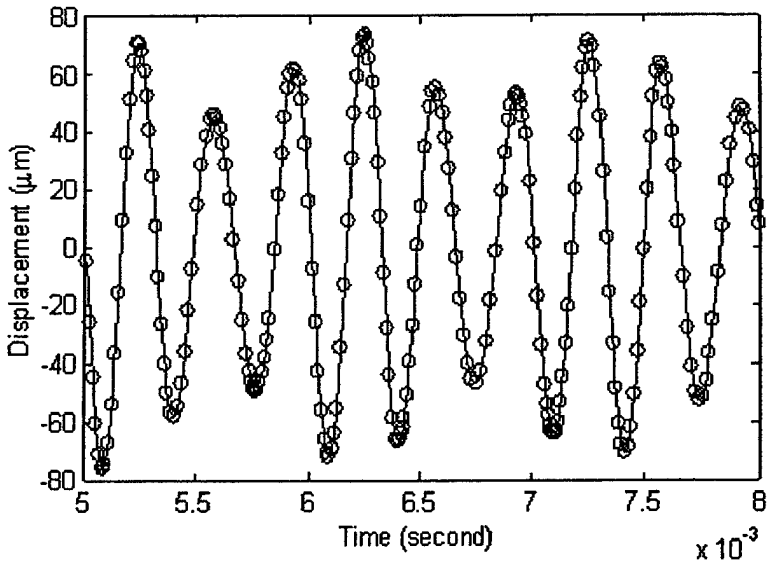

Figure 5: A snap shot of dynamic response when the input is operating at 3000 Hz. The figure highlights the variations in output displacement (y-axis) in each motion cycle.

The spectrum of the phase difference between the output and input is shown in Fig. 6(b). In static and low speed situations, the phase difference is near 180°, coinciding with the intended design result. That is, the input and the output are moving in directions opposite to each other. But when the frequency ratio is over 0.9, the phase difference reduces quickly. At the resonant state, the phase difference is near zero. The input and output move in the same direction. This is exactly opposite of the intended performance. If the reversed phase is necessary for keeping the system working properly, the analysis indicates that the mechanism must operate at frequencies far away from the resonant state either at relatively low frequency or at very high frequencies.

The GA also changes with the operating frequency of the compliant mechanism. It can be seen from Fig. 6(c) that the GA value vacillates around the static design result of 12.1:1. The reason that GA changes with the input frequency is because the amplitudes of the input displacement and output displacement do not change at a constant phase angle when input frequency changes. Therefore, dynamic simulation is needed to determine the actual GA at the operating frequency. For the stroke amplification mechanism, analysis indicates that the desired geometrical advantage 12.1:1 can be maintained as long as the frequency ratio is less than 0.2 or one-fifth the natural frequency.

The sensitivities of the fundamental natural frequency of the stroke amplification compliant mechanism to the mass and bending stiffness of each element are calculated and the results are presented in Fig. 7. Generally, increasing the bending rigidity and reducing the mass of the mechanism will increase the natural frequency because the sensitivity to bending stiffness is

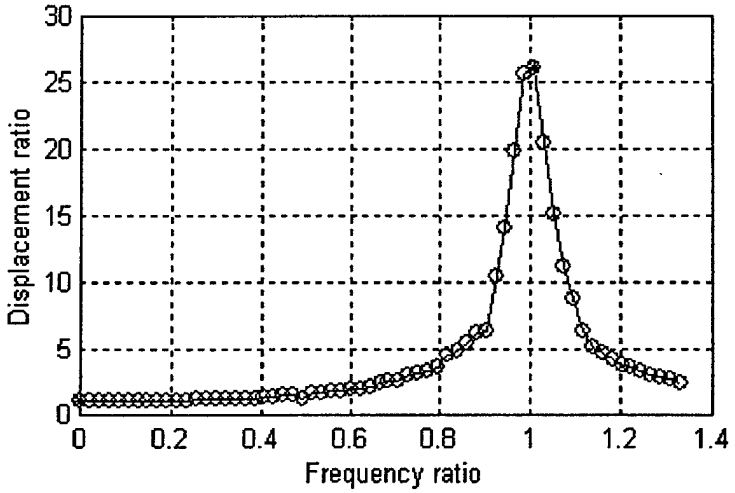

Figure 6(a) Amplitude-frequency characteristic of the stroke multiplier mechanism.

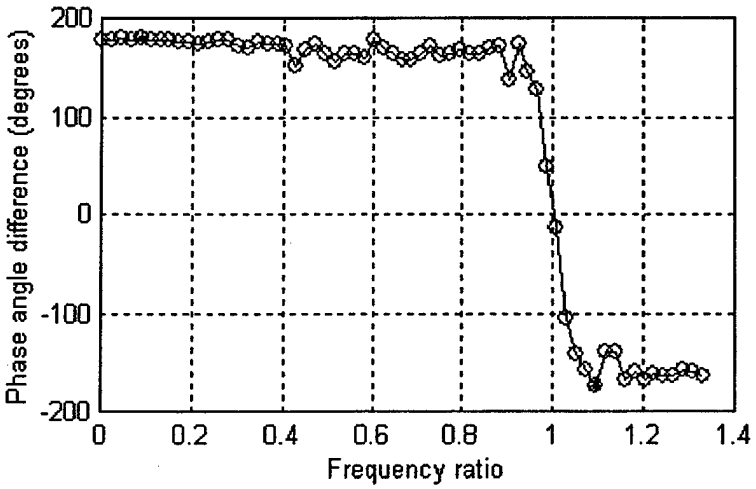

Figure 6(b) Phase-frequency characteristic of the stroke multiplier mechanism.

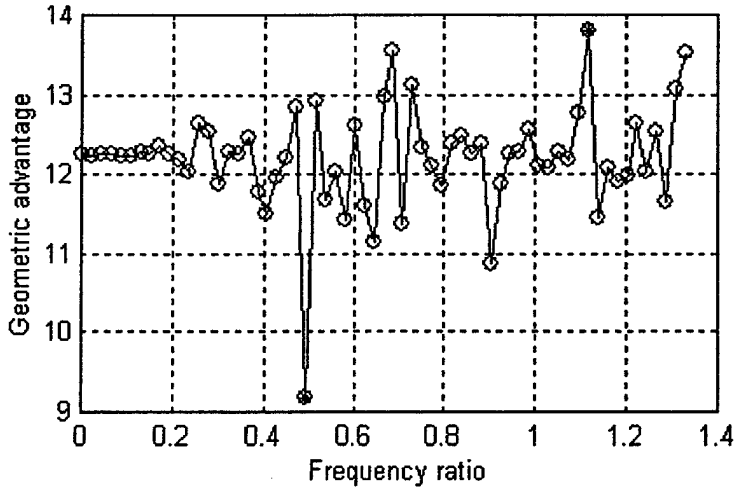

Figure 6(c): Response spectrum of Geometric Advantage of the Stroke Amplifier.

positive, and the sensitivity to the mass is negative. The sensitivity analysis results of Fig. 7, suggest that the most effective means to increase the fundamental frequency of the compliant multiplier (refer to Fig. 2 for element positions) would be to

(a) reduce the mass of elements 15, and/or element 16

(b) reduce the mass of the output port,

(c) increase the bending stiffness of element 14.

This also suggests that the dynamic performance will be less sensitive to manufacturing errors in elements other than the ones noted above. To verify this, we changed the cross-section of element 14 from its original thickness×height of 2.5×1.25(μm) to 1.25×2.5(μm). The mass of element 14 did not change, but the bending stiffness increased by four times. The fundamental natural frequency increased from 3883.24(Hz) to 5192.40(Hz). If the same change was made to element 13 (from original thickness×height = 2.5×1.25(μm) to 1.25×2.5(μm)), the fundamental natural frequency will increase only from 3883.24(Hz) to 3968.51(Hz). The same change on different elements brings very different results. For the same change in geometry, the change in natural frequency was 1223.89(Hz). This demonstrates the effectiveness and necessity of synthesizing a mechanism based on the sensitivity analysis.

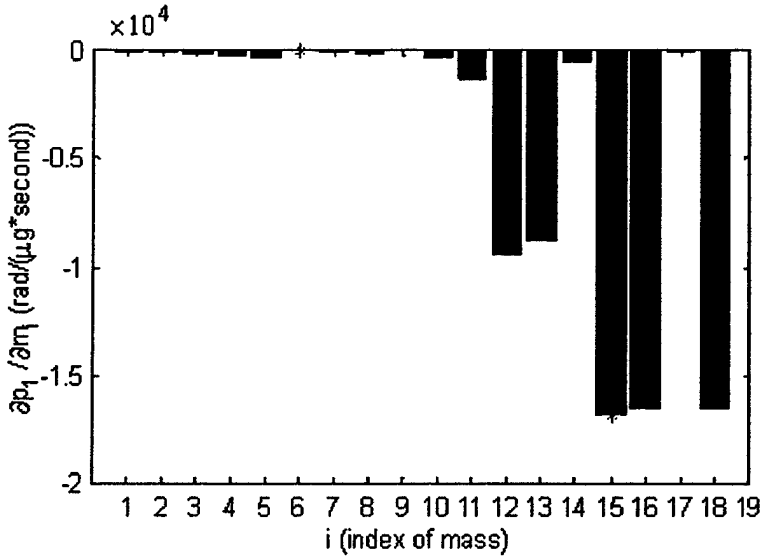

Figure 7(a) Sensitivity of fundamental frequency to the mass of various elements.

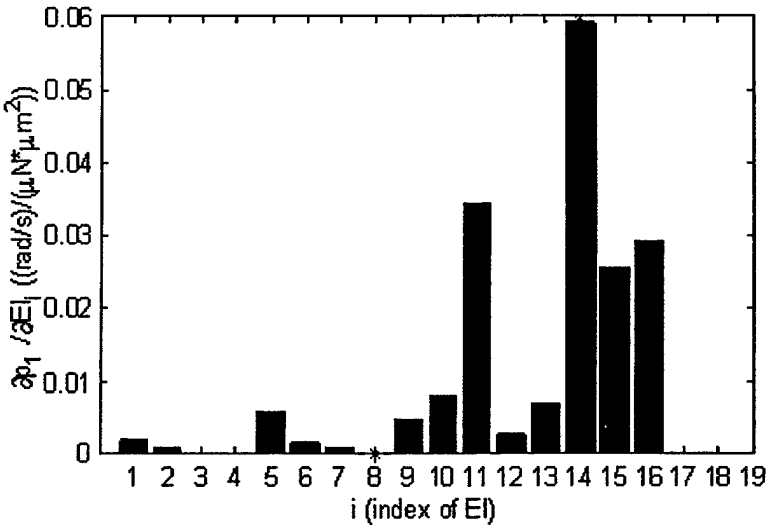

Figure 7(b) Sensitivity of fundamental frequency to the bending stiffness of various elements.

5.5 Dynamic Analysis Software for Compliant Mechanisms

A compliant mechanism design and dynamic analysis software has been developed by the authors using MATLAB. The software can solve for natural frequencies, natural modes, static deformations and stresses, dynamic responses, frequency characteristics, and sensitivities. The main user interface of this dynamic analysis software is shown in Fig. 8. Above results in the numerical example section are obtained by using this analysis tool.

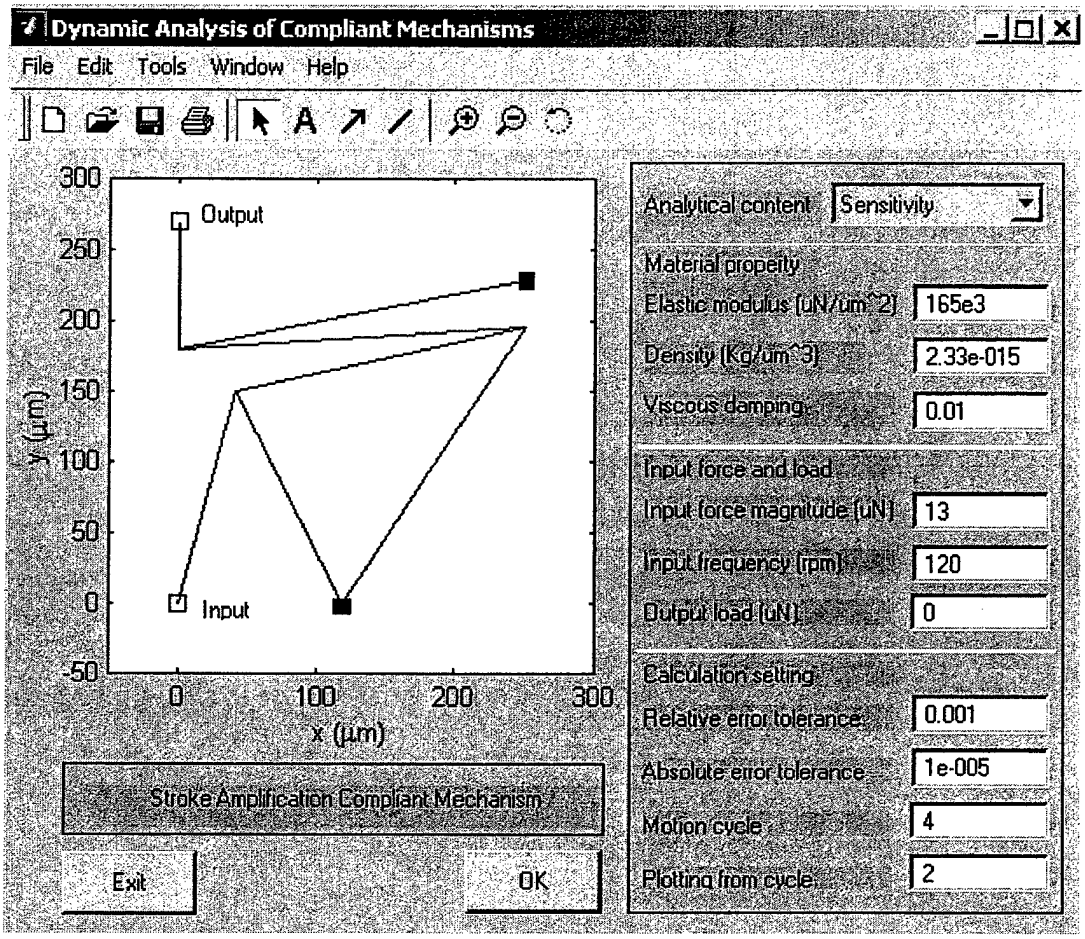

Figure 8: Dynamic Analysis Software developed by Zhe Li and S. Kota, University of Michigan.

5.6 Conclusions

We developed a systematic method for performing dynamic analysis of compliant mechanisms including the basic formulations. The report described the basic elements of dynamic analysis such as natural frequencies, natural modes, dynamic response, frequency spectrum analysis, and sensitivity analysis. The sensitivity analysis method forms the basis for dynamic *synthesis* of compliant mechanisms (future work). The results from our dynamic analysis software were verified experimentally by researchers at the Sandia National Labs for MEMS applications. As illustrated in the design example, differences between static and dynamic behavior of compliant mechanisms can be significant, and they should be accounted for during the design phase.

6.0 REFERENCES

1. Sevak, N.M. and McLarnan, C.W., "Optimal Synthesis of Flexible Link Mechanisms with Large Static Deflections," ASME Paper No. 74-DET-83 (1974).
2. Howell, L.L. and Midha, A., "A Method for the Design of Compliant Mechanisms With Small-Length Flexural Pivots," ASME *Journal of Mechanical Design* **116**, (1994) 280-290.
3. Tuttle, S.B., "Chapter 8, Semifixed Flexural Mechanisms," *Mechanisms for Engineering Design*, John Wiley and Sons, Inc., New York, 1967.
4. Paros, J. and Weisbord, L., "How to Design Flexible Hinges," *Machine design*, Nov. 25, (1965) 151-156.
5. Shoup, T.E., "On the Use of the Nodal Elastica for the Analysis of Flexible Link Devices," ASME *Journal of Engineering for Industry*, **94**(3), (1972) 871-875.
6. Murphy, M.D., Midha, A. and Howell, L.L., "The Topological Synthesis of Compliant Mechanisms," *Mechanism Machine Theory*, **31**(3), (1996) 185-199.
7. Ananthasuresh, G., Kota, S. and Kikuchi, N., "Strategies for Systematic Synthesis of Compliant MEMS," *Dynamic Systems and Control*, DSC-Vol.55-2, ASME Annual Meeting, Chicago, IL, (1994) 677-868.
8. Frecker, M., Ananthasuresh,G., Kikuchi, N. and Kota, S., "Topological Synthesis of Compliant Mechanisms Using Multi-Criteria Optimization," ASME *Journal of Mechanical Design,* **119**, (1997) 238-245.
9. Larsen, U., Sigmund, O. and Bouwstra, S., "Design and Fabrication of Compliant Micromechanisms and Structures with Negative Poisson's Ratio," *Journal of Microelectromechanical Systems*, **6**(2), (1997) 99-106.
10. Hetrick, J. and Kota, S., "An Energy Formulation for Parametric Size and Shape Optimization of Compliant Mechanisms," ASME *Journal of Mechanical Design,* **121**, (1999) 229-234.
11. Joo, J., Kota, S., and Kikuchi, N., "Nonlinear Synthesis of Compliant Mechanisms: Topology Design," ASME Paper No. DETC2000/MECH-14141 (2000).
12. Chandrupatla, T.R., Belegundu, A.D., *Introduction to Finite Elements in Engineering,* Prentice Hall, Inc., Upper Saddle River, NJ, 1997.

13. Cook, R.D., *Concepts and Applications of Finite Element Analysis*, John Wiley & Sons, Inc., New York, 1981.
14. Shabana, A.A., Vibration of Discrete and Continuous Systems, Springer-Verlag New York, Inc., New York, 1997.
15. Midha, A., Erdman, A.G., and Forhrib, D.A., "Finite Element Approach to Mathematical Modeling of High-Speed Elastic Linkages," *Mechanism and Machine Theory*, **13**, (1978) 603-618.
16. Ewins, D.J., *Modal Testing: Theory and Practice*, John Wiley & Sons, Inc., New York, 1984.
17. Weck, M., *Handbook of Machine Tools, Vol. 4, Metrological Analysis and Performance Tests*, John Wiley & Sons, Inc., New York, 1984.
18. Brigham, E.O., *The Fast Fourier Transform and Its Applications*, Prentice Hall, Inc., Englewood Cliffs, NJ, 1988.